Swelling-induced morphology in ultrathin supported films of poly(*d*,*l*-lactide)

J. S. Sharp[1,*] and R. A. L. Jones[2]
[1]*Department of Physics, University of Waterloo, 200 University Avenue West, Waterloo, Ontario, Canada, N2L 3G1*
[2]*Department of Physics and Astronomy, University of Sheffield, Hounsfield Road, Sheffield, S3 7RH, England*
(Received 12 December 2001; published 25 July 2002)

In this study we describe a surface morphology that arises when ultrathin supported films of poly(*d*,*l*-lactide) are immersed in water. The films are initially flat with a rms roughness of approximately 2 nm. After immersion the surfaces of the films are covered with craters. The craters have a narrow distribution of sizes and are typically micrometers in diameter. They have depths in the 10–100 nm range. *In situ* atomic force microscopy shows that the craters occur as a result of a blistering process, which occurs when the films delaminate from the silicon substrate. The films buckle away from the substrate to give a nonzero initial diameter and then the blisters proceed to grow until they reach a maximum size. At any point during the growth process, the blisters can be made to collapse by removing the films from water. This phenomenon is explained in terms of a laterally confined swelling film, which has a buckling instability and releases excess strain energy by wrinkling. An expression for the initial buckling wavelength is extracted using the expressions for a buckling plate. Information about the mechanical properties of the films and the surface interaction between the film and substrate can also be obtained by considering the kinetics of blister growth.

DOI: 10.1103/PhysRevE.66.011801 PACS number(s): 68.60.−p, 68.55.−a, 68.90.+g

INTRODUCTION

Systems that display spontaneous, surface directed, pattern formation have attracted a lot of interest in recent years [1–5]. These types of process can be used to produce structures on the micrometer and submicrometer length scales and have potential applications for the production of templates for integrated circuits and coatings with tailored optical properties [6]. The length scales in these systems typically arise as a result of a competition between two or more different processes [2–4]. One of these processes usually favors long wavelength structures while the other favors short ones. When the experimental conditions are adjusted and the system is allowed to evolve, all the wavelengths initially have similar contributions. However, as time progresses the competing mechanisms result in the selection of a characteristic wavelength which grows at the expense of others.

In this work we describe how ultrathin films of a low molecular weight aliphatic polyester [poly(*d*,*l*-lactide)] can be made to delaminate from a single crystal silicon substrate by immersing them in water at elevated temperatures. A balance between the swelling stresses in the unbuckled film and the bending stresses in the buckled part of the film results in the selection of a characteristic blistering length. The films used in this study were initially flat with a rms roughness of approximately 2 nm, but when immersed in water the films blister away from the substrate. When removed from water and dried the blisters collapse to form craters which have similar diameters to the original blisters and are tens to hundreds of nanometers deep. The procedure of simply immersing a spun cast polylactide film in warm water therefore represents a simple and inexpensive route for the production of structures on some interesting size scales. The mechanisms responsible for blistering of the polymer film are not unique to this system and we expect that the blistering phenomenon described here could be observed in other polymer/solvent systems.

The delamination or debonding of coatings from a substrate is important for many applications. This type of phenomenon is important in understanding how paint peels off metal surfaces when damage or corrosion of the underlying surface takes place [7]. It is also necessary to understand these processes when producing flexible thin film transistors, where the multilayers can detach if the device is bent through a small radius of curvature [8].

Delamination usually occurs as a result of thermal, bending, or swelling stresses which arise when the coating is exposed to heat, placed under compressive load, or swollen in a solvent [9,13]. The coatings used often have different physical properties to the underlying substrate. These properties include quantities such as the thermal expansion coefficients and Young's moduli. The coating may also have a different swelling response than the substrate to a particular solvent. A mismatch in these types of property results in the coating being left in a state of strain (extension or compression) when the film and substrate are heated, bent, or immersed in solvent.

For the case of bending, if the stresses in the film are large enough to overcome the adhesion forces between the film and substrate, then the interface between the two materials will fail and the film will start to delaminate [8]. This usually occurs at a defect on the interface.

When the films are supported on a substrate and either heated or swollen in solvent, then the film can expand freely out of the plane of the film, but becomes confined laterally. If the lateral stresses in the film exceed a critical value, then an instability is created which causes the coating to buckle away from the substrate and delaminate.

In both these cases, there exist regions of the film that do not initially detach from the substrate and that remain in a

*Author to whom correspondence should be addressed. Email address: jssharp@sciborg.uwaterloo.ca

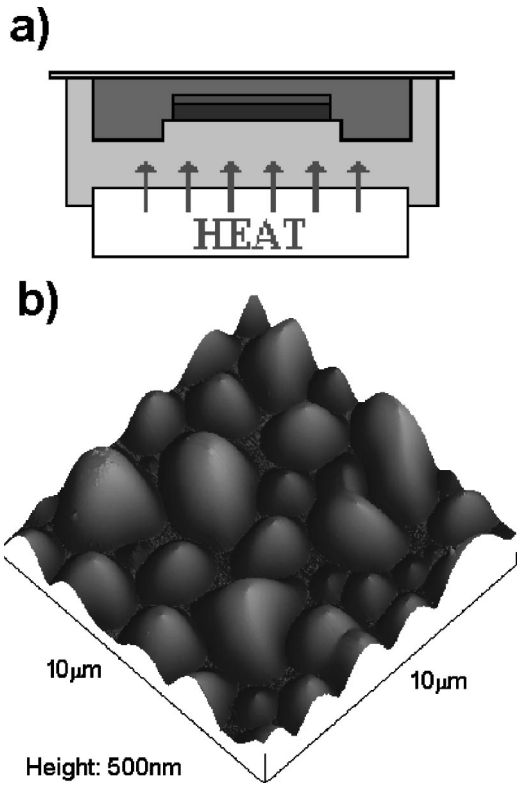

FIG. 1. (a) The water bath used for swelling the polymer films at constant temperature consists of a piece of aluminium machined to fit on top of a Linkam hot stage, which can be filled with water and covered with a glass cover slip. A T type thermocouple is used to measure the temperature of the water. (b) Samples immersed in water at 40 ° C buckle away from the substrate to form blisters. These blisters grow and coalesce until they reach a maximum size. An AFM image is shown for a 150 nm thick film (size 10 $\times 10$ μm; height 500 nm) that has been immersed for 5 min.

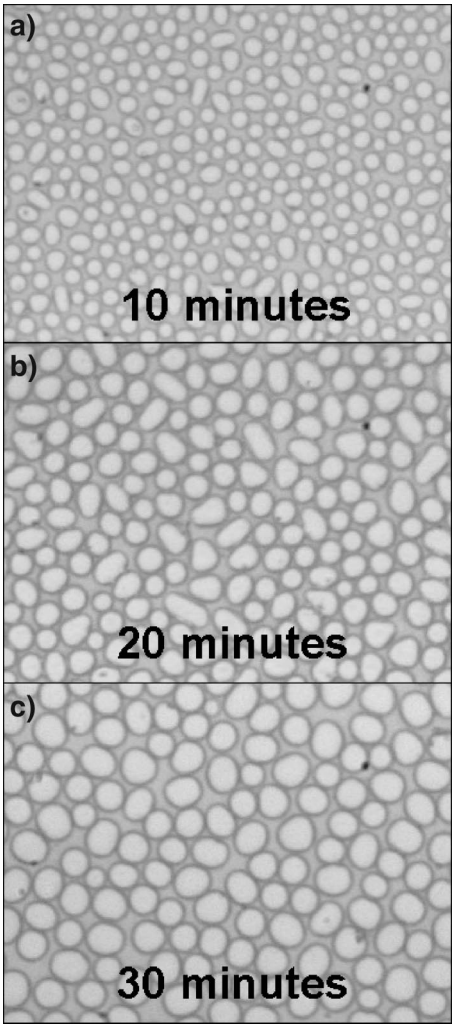

FIG. 2. Samples immersed in water for different times, removed, and dried, show how the blisters grow. Optical micrographs are shown for 200 nm films immersed in water at 40 °C for (a) 10 min, (b) 20 min, and (c) 30 min.

state of strain. As a result, the newly formed blisters grow to release the excess strain energy. The process of blister growth has been extensively studied and is well described by fracture mechanics theories [9–12]. A wealth of literature is also available that describes the experimental contributions made to the field and an excellent summary of the observed blistering morphologies that have been reported to date can be found in the papers by Gioia and Ortiz [10,11].

The circular blistered structures reported in this work form a small subclass of the wide range of blistering morphologies that have been observed experimentally. However, to our knowledge, this work represents the first incidence of a swelling polymer film being used to produce a periodic buckling structure. The uniform stress field provided by the rapid swelling of the polymer, coupled with weak adhesive forces between the film and substrate, means that the system buckles everywhere on the surface of the film to produce a series of blisters with a mondisperse distribution of diameters, similar to those predicted by Pomeau [12]. Residual stresses in the unbuckled areas of the film then cause the blisters to grow. However, blistering is not the only mechanism by which the films can release stored strain energy. Flow of the polymer chains also allows the film to relax some of the swelling stresses, so the films grow until sufficient stress in the film has been dissipated and the work done by the stresses in the film becomes insufficient to overcome the adhesion energy between the film and the substrate. In this sense, the blistering of a viscoelastic film differs from that of the studies of elastic films described by Ortiz and Gioia. A simplified theory is derived to explain these stress dissipation phenomena and to explain why blisters on a film of a particular thickness stop growing.

The flow of the swollen polymer also results in an increase in the area of the blistered parts of the film, such that when the blisters are removed from water they collapse and wrinkle to form craters with a monodisperse distribution of sizes and with similar depths. The craters produced can also be made to form well ordered arrays, simply by gently rubbing the substrate prior to deposition of the films. The ability to produce an ordered array of micrometer sized craters by simply immersing a polymer film in water is potentially very exciting and has a number of applications, some of which have been suggested above.

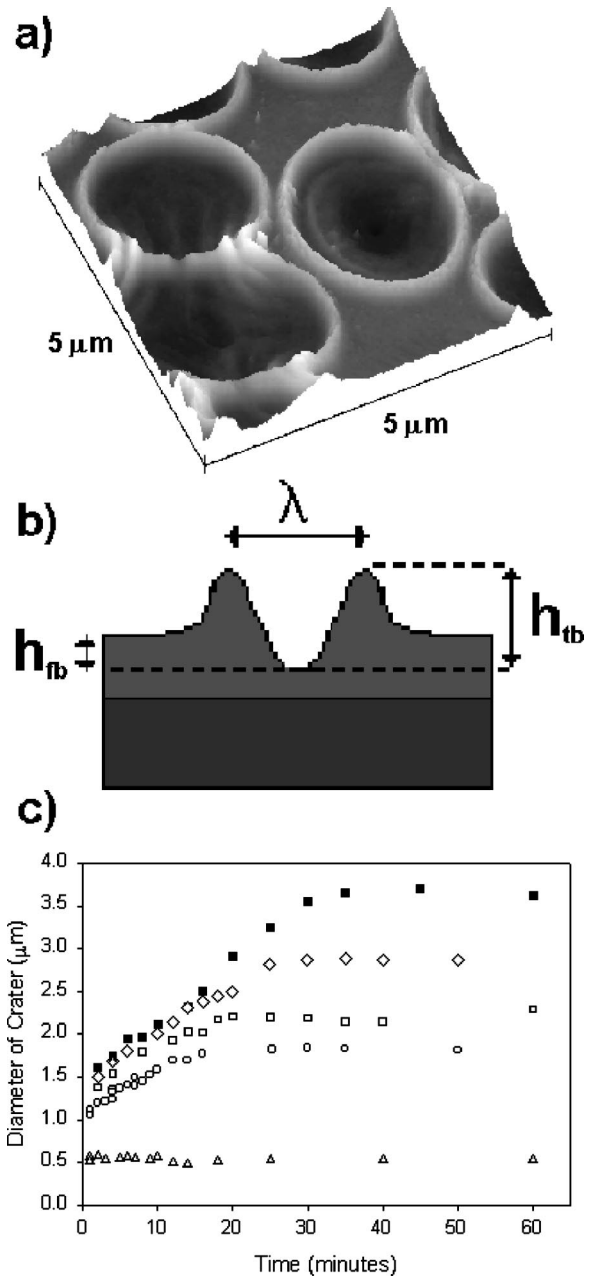

FIG. 3. (a) Removing the films from water causes the blisters to collapse and form craters. As the polymer collapses back to the substrate, it wrinkles, producing the rings shown in the image. (b) Measurements of the diameter and depth of the craters were taken using an optical microscope and an atomic force microscope. (c) Crater growth curves. Data are shown for films immersed in water at 40°C. The film thicknesses shown are (△) 50 nm, (O) 100 nm, (□) 150 nm, (◇) 190 nm, and (■) 200 nm.

EXPERIMENT

The polymer used in this study was a low molecular weight (12 kDa) polyester, called poly(*d*,*l*-lactide) (PLA). Supported films were made by spin coating the polymer from solutions in chloroform on to 1 cm^2 substrates of single crystal silicon and annealing at 40°C for 1 h. The silicon used was obtained from Compart technology and had been cleaved parallel to the [100] axis. Each substrate had a natural oxide coating that was typically 1.8 nm thick. The polymer was obtained from AstraZeneca (U.K.) Ltd. The thickness of the polymer films was measured using ellipsometry. The range of thicknesses studied was 22–300 nm. Roughness measurements were also taken on the annealed films using the atomic force microscope (AFM) and the rms roughness typically found to be 0.5 nm.

After annealing, the supported polymer films were placed individually into a specially constructed water bath. The bath consisted of a piece of aluminum machined so that it could be mounted onto a Linkam hot stage [see Fig. 1(a)], filled with water and covered with a glass cover slip. The films were immersed for different times at a range of temperatures, so that both kinetic and temperature dependent data could be obtained. A thermocouple was introduced through a hole in the side of the bath, so that the temperature could be measured independently. The temperature stability was found to be ± 1 °C at 40°C . After immersion, the films were removed and gently dried with nitrogen gas.

The samples were imaged using a Nikon Eclipse ME600 optical microscope and a Digital Instruments Multi Mode atomic force microscope with a Nanoscope IIa controller. Both were equipped with image analysis software. This allowed for the measurement of both the lateral dimensions and depths of any surface features. Between 100 and 200 objects were imaged on each sample.

RESULTS

In situ AFM of the sample placed in water at 40 °C showed that the films were blistering away from the substrate [Fig. 1(b)]. As time progressed, these blisters grew and coalesced until they reached a maximum diameter. An AFM tip was used to puncture one of the blisters to test if the films were delaminating at the polymer silicon interface. The resulting AFM image showed that the difference in height between the bottom of the ruptured blister and the top of the unblistered parts of the film was equal to the film thickness. This indicates that failure of the polymer-silicon interface is occuring during blister production and that internal failure of the polymer film is not taking place.

Samples that had been immersed in water and removed were observed to be covered with a monodisperse distribution of craters. The optical microscope, equipped with IMAGE-PRO PLUS software (Media Cybernetics), was used to measure the size of the features (Fig. 2) and some of the samples were also imaged using the AFM [Fig. 3(a)]. The measurements taken are shown in Fig. 3(b). These include the blistering length λ, the distance between the top of the crater and its base, h_{tb}, and the distance between the top surface of the film and the crater base, h_{fb}. In all cases the blisters on the films were observed to be present everywhere on the surface and had collapsed and wrinkled to form craters. When imaged with the AFM, the craters were found to be completely lined with polymer, indicating that rupturing of the blisters does not occur when they are removed from the water.

Growth curves were constructed for the craters by immersing samples of the same thickness in water for different

periods of time at 40°C and imaging them with the optical microscope [see Fig. 3(c)]. This was done for films that were 22, 32, 50, 100, 150, 190, and 200 nm thick.

DISCUSSION

Buckling of confined systems

The most familiar buckling problem is that of the thin beam. This assumes that a beam of length l is unsupported and has a force F applied to the ends of the beam (see Fig. 4). In this case the beam is laterally confined and is stable until the force exceeds a critical value F_c, which is related to the length l moment of inertia, I, and Young's modulus E of the beam and is given by

$$F_c = \frac{n^2 \pi^2 EI}{l^2,} \quad n = 1,2,3, \ldots . \tag{1}$$

For $F < F_c$, the beam remains horizontal and there is no vertical deflection, and for $F \geqslant F_c$ the beam buckles as shown in Fig. 4. In this case the critical stress is set by the length of the beam. In practice, the only buckling mode that is excited is the first $(n=1)$, as this is always the first one reached when a force is applied. However, it is possible to excite higher buckling modes by instantaneously applying a large enough force to do so and by supporting the beam at the deflection nodes [14].

The theories that deal with the analysis of buckling plates are well understood and are dealt with in a few specialist texts [15–17]. As well as dealing with unsupported plates, some authors have considered the case of a plate which is rigidly attached to a substrate [18,19]. In these systems, the plate/film was applied to a thick substrate and subjected to some form of stress. Allen [18] describes how sandwich panels buckle when an axial load is applied, illustrating that it is possible for large supported plates to wrinkle with wavelengths that are much smaller than the length of the panel. This can occur for stresses that are smaller than the critical stress required to buckle the whole structure.

Bowden *et al.* [19] illustrated that this was possible by evaporating a metal layer a few nanometers thick onto one side of a ''thick'' PDMS [poly(dimethylsiloxane)] film. During the evaporation, the temperature of the PDMS film increased, causing it to expand. When the metal coated polymer was removed and subsequently cooled, the mismatch in expansion coefficients between the metal and polymer caused wrinkling of the gold film with a wavelength that was very much smaller than the length of the PDMS substrate.

In the systems described by Allen [18] and Bowden *et al.* [19], it is clear that the adhesion of the thin films to the thicker substrates plays some role in producing a buckled structure which has a short wavelength and which is formed at stresses that are lower than those required to buckle the whole structure. In the first case, the adhesion between the sandwich panels and the substrate prevents the sandwich plates from debonding when placed under load, so that the mismatch in the Young's moduli of the two materials causes them to be compressed by different amounts, giving rise to a wrinkling instability. The second case is very similar, except that the adhesion between the film and substrate combined with a mismatch in the expansion coefficients of film and substrate gives rise to the short wavelengths observed.

The analysis in the above cases assumes a soft substrate coated by a rigid overlayer. In the work presented here, the system under study consists of a rigid substrate coated by a ''softer'' polymer overlayer. However, the films still buckle with a wavelength that is much smaller than the size of the sample.

When a film is immersed in solvent, it swells and can be treated as an elastic plate with a homogeneous stress distribution in the plane of the plate. The stresses arise because the film tries to expand but is confined by the substrate. If these stresses exceed a critical value the film will buckle with a half wavelength λ, that is determined by considering the balance between the membrane stresses in the unbuckled film, the bending stresses in the buckled state, and the forces required to overcome the adhesion of the film to the substrate.

In the case of zero or negligible adhesion forces between the film and substrate, the wavelength is simply determined by a competition between the membrane stresses in the film created by confining the swelling system and the bending stresses that arise when the film becomes buckled. The problem can be approached by considering the system as a plate which is held under biaxial load (provided by the swelling stresses σ in the film). The governing equation is simply given by [15]

$$D\left(\frac{\partial^4 w}{\partial x^4} + 2\frac{\partial^4 w}{\partial x^2 \partial y^2} + \frac{\partial^4 w}{\partial y^4}\right) = S_x \frac{\partial^2 w}{\partial x^2} + S_y \frac{\partial^2 w}{\partial y^2}, \tag{2}$$

where w is the deflection of the plate away from the substrate at the coordinate (x,y) and D is the *flexural rigidity* (or resistance to bending) of the plate, defined as $D = Eh^3/12(1-\nu^2)$ with E being the Young's modulus of the plate material, ν the Poisson ratio, and h the plate thickness. The quantities S_x and S_y are the forces acting per unit length in the plane of the plate, due to the swelling stresses. For a homogeneous stress distribution these can be rewritten as $S_x = S_y = \sigma h$. Inserting these results into Eq. (2) gives

$$\frac{Eh^2}{12(1-\nu^2)}\left(\frac{\partial^4 w}{\partial x^4} + 2\frac{\partial^4 w}{\partial x^2 \partial y^2} + \frac{\partial^4 w}{\partial y^4}\right) = \sigma\left(\frac{\partial^2 w}{\partial x^2} + \frac{\partial^2 w}{\partial y^2}\right). \tag{3}$$

By examination, a solution to Eq. (3) can be obtained by using a product of trigonometric functions of the form

$$w = w_0 \sin\left(\frac{\pi x}{l_1}\right)\sin\left(\frac{\pi y}{l_2}\right).$$

The high level of symmetry observed in the blisters allows us to write that $l_1 = l_2 = \lambda$. Inserting these results into Eq. (3) and rearranging gives

FIG. 4. When a force F is applied to the ends of a beam it remains horizontal until the force exceeds a critical value F_c.

$$\lambda = \pi h \left(\frac{E}{6\sigma(1-\nu^2)} \right)^{1/2} = \pi h \left(\frac{1}{6\epsilon_{lin}} \right)^{1/2} \tag{4}$$

where ϵ_{lin} is the strain imposed on the plate in one dimension. The above form is very similar to that derived by Pomeau [12] for a thin plate under biaxial stress.

The linear strain ϵ_{lin} can be written in terms of the equilibrium volume fraction of solvent ϕ in the swollen plate, by assuming that the strain in each dimension is the same. Doing this yields the result that $\epsilon_{lin} = \phi/3(1-\phi)$.

The equilibrium volume fraction of water in poly(d,l-lactide) was determined by immersing a bulk sample in water at 40 °C and weighing it until there was no change in the mass. The value obtained at this temperature was $\phi = 0.115$.

By inserting the above results into Eq. (4) and extrapolating the curves in Fig. 3(c) to zero time, it is possible to make a comparison between experiment and the simple theory. The results are plotted in Fig. 5 with the predictions of the simple theory being given by the dashed line.

The main assumptions of this simple theory are that the lateral dimensions of the film are very much greater than the thickness of the plate and that the strain imposed is instantaneously applied and is uniform throughout the plate material. The first assumption holds because the lateral dimensions of the films used were typically 1 cm and the thickest samples used were around 300 nm thick (a factor of 10^5 difference). The second assumption can only be assumed to hold if the equilibration time of the solvent volume fraction inside the film is much smaller than the experimental time scale. Using the approximate expression for the width of the concentration profile x produced as a result of solvent diffusion,

$$\langle x^2 \rangle \sim Dt,$$

the equilibration time t_{eq} is given by the equation,

$$t_{eq} \sim \frac{h^2}{D},$$

where h is the film thickness and D is the diffusion coefficient of the solvent in the polymer.

The diffusion coefficient of water in PLA at 40 °C was measured by immersing a 1 mm thick film of the polymer in water and removing it at regular intervals for weighing. The mass uptake profile was then fitted to a Fickian model and the diffusion coefficient was determined to be 2.53×10^{-11} m^2 s^{-1}. Inserting this value in the equation above, along with a typical thickness (300 nm), gives an equilibration time of $t_{eq} \approx 10^{-3}$ s. This is much faster than the experimental time scale and so the assumption of a uniform stress field at early times holds.

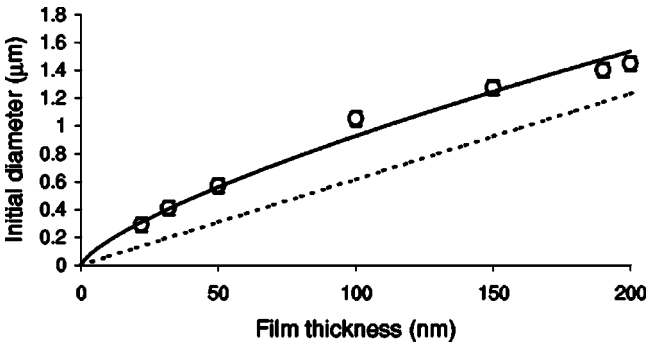

FIG. 5. Comparison of the initial diameter λ of the craters with the predictions of Eq. (4) (dashed line) for the case of no adhesion. Data were obtained by extrapolating the curves in Fig. 3(c) to time $t = 0$. The solid line shows the best power law fit ($h^{3/4}$).

It is clear from Fig. 5 that the simple theory correctly predicts the order of magnitude of the blister and subsequent crater diameters. However, it does not predict the functional form of the dependence of the crater diameter upon thickness. The power law that best fits the shape of the data varies as $\lambda \approx h^{3/4}$ instead of the linear form predicted by Eq. (4).

Adhesion between the film and substrate is likely to affect the blistering wavelength and it is clear that it plays a role in these experiments because the films remain attached to the substrate. The swelling of the polymer causes local debonding of the film and substrate and some work has to be done to overcome the local adhesive forces. This local detachment of the film is believed to be due to defects at the film-substrate interface [9]. These localized delaminating sections of the film behave like small individual plates that are clamped by the substrate, but which then have this restriction removed to be allowed to grow. Using energy conservation arguements for the film at the point of buckling, the effective strain energy per unit area is given by $\frac{1}{2}[E/(1-\nu^2)]\epsilon_{eff}^2 h = \frac{1}{2}[E/(1-\nu^2)]\epsilon^2 h - \Gamma$, where Γ is the adhesion energy per unit area of the film to the substrate.

This reduction in the effective strain in the film would cause an increase in the wavelength of the blisters according to Eq. (4). So the blistering length λ is pushed to slightly higher wavelengths than those predicted by the simple theory. The increase in the blistering wavelength arises because the reduction in strain energy means that there is less energy available to bend the film and short wavelength wrinkles have a higher bending energy penalty than longer wavelength ones. A simple form for the blistering length cannot be obtained by using a modification of the existing theory and a more complicated approach is required to describe the effects introduced by adhesion.

Growth kinetics

After the initial buckling, the driving force for blister growth arises because there are still areas of the film which remain attached to the substrate and which are still in a state of strain. Growth of the blister releases some of this strain energy, but also creates more surface. This requires that work be done to overcome the adhesive forces between the film and substrate. Local bending stresses in the blistered part of

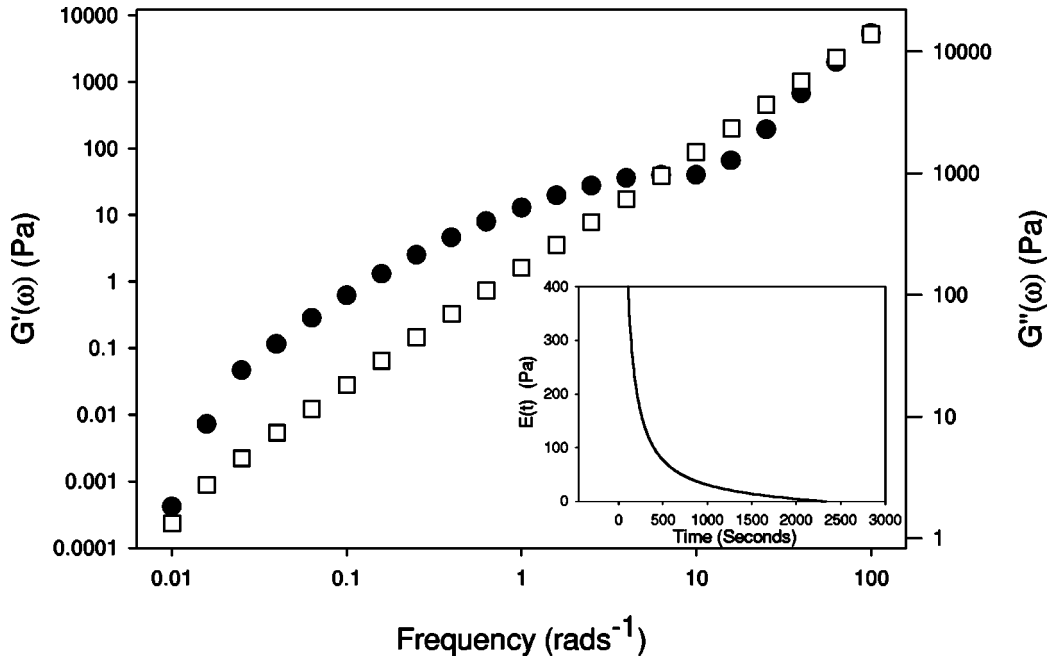

FIG. 6. The rheological properties of fully hydrated poly(d,l-lactide) at 40 °C. The data shown are for the real $[G'(\omega)]$ (●) and imaginary $[G''(\omega)]$(□) parts of the frequency dependent modulus. Inset is the time dependent modulus $E(t)$, obtained by Fourier transforming $G'(\omega)+iG''(\omega)$ over the frequency range of the data.

the film can be considered small except at the crack tip where the film is still attached to the substrate. Here the stresses are quite high and allow the crack tip to propagate and produce more free surface [20]. For the most part the contributions from the buckled part of the film can be neglected except to say that the crack tip is allowed to propagate because of these stress concentrations. Fracture mechanics provides a simple expression for the rate of energy release G with respect to changes in the blister area A [9]. Assuming a circular blister gives the expression

$$G=\frac{1}{2\pi a}\frac{dU}{da}=\frac{1}{2}E\epsilon^2h-\Gamma. \tag{5}$$

This equation shows that if $\frac{1}{2}E\epsilon^2h\leqslant\Gamma$ then G is negative or zero and the blister will not grow. This is also the condition that determines whether or not the film will blister, because if the strain energy is insufficient to overcome the energy of adhesion the film will not detach from the substrate. However, when $\frac{1}{2}E\epsilon^2h>\Gamma$, the energy release rate G is always positive and Eq. (5) shows that as the area of the blister increases the rate of energy release also increases. For a film that remains in a constant state of strain, this means that the blisters will grow until the whole film is removed from the substrate. This clearly does not happen, because the crater diameters shown in Fig. 3(c) stop increasing after some time τ_0, which appears to depend on the film thickness. This is believed to be due to viscous flow of the material within the film in response to the applied swelling stresses. It is clear that some viscous flow does occur in the films, because the base of the craters was always measured to be lower than the top of the film, indicating that some thinning of the film had occurred during the experiments.

The relevant time scale for the flow of material in the blistering experiments ranges from minutes to tens of minutes. This corresponds to a range of frequencies equivalent to 0.01–0.1 Hz. Figure 6 shows how the rheological properties of fully hydrated PLA vary with the frequency of the applied shear. These measurements were performed on a Rheometrics Scientific SR5000 stress controlled rheometer with a cone and plate geometry, using a 1 mm thick sample and a stress of 100 Pa. The inset in Fig. 6 is a plot of the stress relaxation modulus $E(t)$. This is obtained by Fourier transforming the quantity $G'(\omega)+iG''(\omega)$ constructed using the data in the main plot of Fig. 6, and is best described by the sum of two negative exponentials, having decay times of 81.4 s and 556.4 s, respectively.

Assuming that the longer time process dominates the form

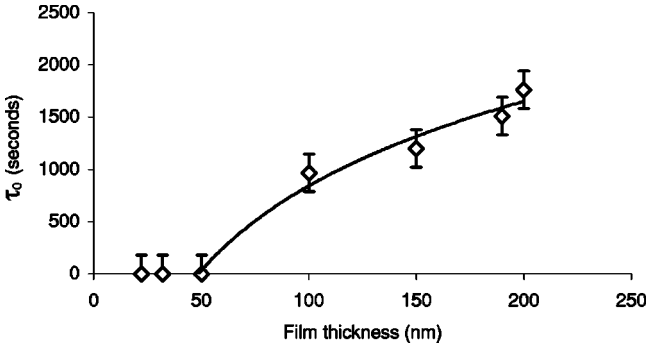

FIG. 7. Comparison of the data collected for the time τ_0 taken for the blisters to stop growing with the form of Eq. (6). τ_0 shows the predicted logarithmic dependence upon the film thickness, but Eq. (6) predicts a cutoff below which blistering should not occur. This is not observed.

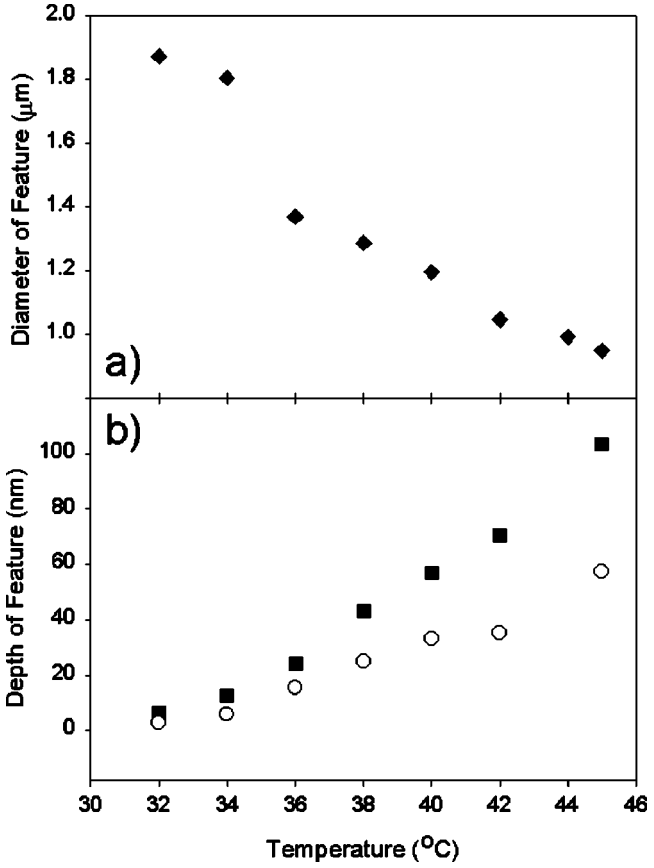

FIG. 8. (a) Temperature dependence of crater diameter. As the temperature increases a reduction in the crater diameter is observed. Data are shown for 90 nm films that have been immersed in water for 5 min. (b) Swelling stresses in the buckled part of the film cause the polymer to flow and thin. Increasing the temperature reduces the viscosity of the polymer, so that a greater amount of thinning occurs for a given stress. The result is a deeper crater when the blisters collapse. Data are shown for 90 nm films that have been immersed in water for 5 min. for both the crater base-to-top distance, h_{tb} (■), and the film-to-base distance h_{fb} (○).

of $E(t)$, the decay of stress in the films can be approximated to a single time relaxation process, so that $E(t) = E_0 \exp(-t/T)$, where T is the relaxation time of the system. The corresponding strain energy per unit area in the film therefore takes the form $U_{strain} = \frac{1}{2} E_0 \exp(-t/T) \epsilon_0^2 h$.

The condition for blister growth is that this strain energy is greater than the adhesion energy between the film and substrate. So the time τ_0 taken for the blisters to stop growing is given by inserting the time dependent strain energy in Eq. (5) and setting the energy release rate G to zero. Rearranging the resulting expression gives a logarithmic form for τ_0 as a function of film thickness:

$$\tau_0 = T \ln\left(\frac{E_0 \epsilon^2 h}{2\Gamma}\right). \tag{6}$$

A fit of Eq. (6) is shown in Fig. 7. There is good agreement between the data and the results of Eq. (6), indicating that the simple model used to describe the decay of stress in the film is correct, at least on a phenomenological level. The curve clearly shows that there is a cutoff below which the blisters should not form or grow. However, Fig. 5 shows that blistering of the films does occur below 50 nm. The reason for this is not completely understood.

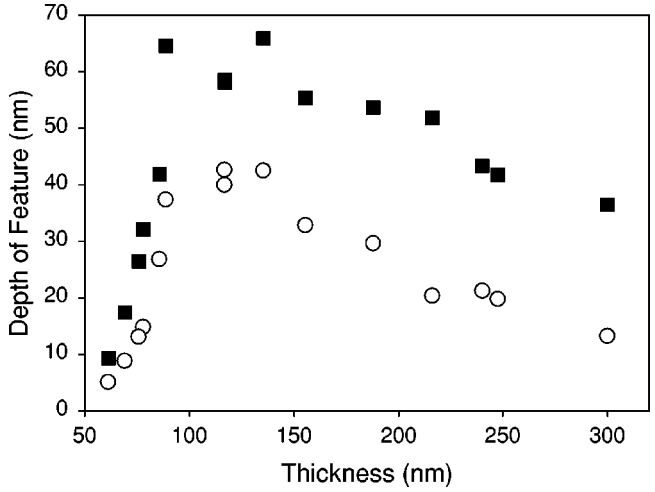

FIG. 9. Variation of depth of craters with film thickness for films immersed in water at 40 °C for 5 min. Data are shown for both the crater base-to-top distance, h_{tb} (■) and the film-to-base distance h_{fb} (○).

Using the fit in Fig. 7 it is possible to extract some of the quantities in Eq. (6). The first of these quantities is the relaxation time T of the polymer. Doing this gives a value of $T = 1650.3$ s, which is comparable to the longer relaxation time of 556.4 s obtained from the fit to the stress relaxation modulus extracted above.

The second quantity that can be obtained from the fit in Fig. 7 is the ratio of the surface energy to the Young's modulus Γ/E. The value extracted from the fit corresponds to a value of $\Gamma/E = 6.07 \times 10^{-5}$ m. Using the value of $E = 0.6$ Pa obtained for a shearing frequency of 0.1 Hz, the value for the surface energy is $\Gamma = 36$ μJ m^{-2} at 40 °C. This value is small when compared to the surface energy of, say, a polymer melt, which typically have surface energies of the order of 10–100 mJ m^{-2} [21] and is more consistent with the interfacial energy of a polymer/solvent interface [22]. The measured value does not actually represent a surface energy; rather it represents the increase in free energy per unit area caused by going from having a PLA/silicon interface to a system where we have PLA/water/silicon, so that $\Gamma = \gamma_{pw} + \gamma_{sw} - \gamma_{ps}$, where γ_{pw}, γ_{sw}, and γ_{ps} are the interfacial energies of the polymer/water, silicon/water, and polymer/silicon interfaces, respectively. This may explain why the value is low compared to the surface energies of polymer melts.

Temperature dependent studies were also performed. These involved immersing 90 nm thick films in water at various temperatures for 5 min. Each sample was then measured on the microscope [Fig. 8(a)]. The data show that as the temperature of the water and sample are increased the size of the blisters decreases.

This is consistent with the predictions of Eq. (4) since an increase in temperature in this material causes an increase in

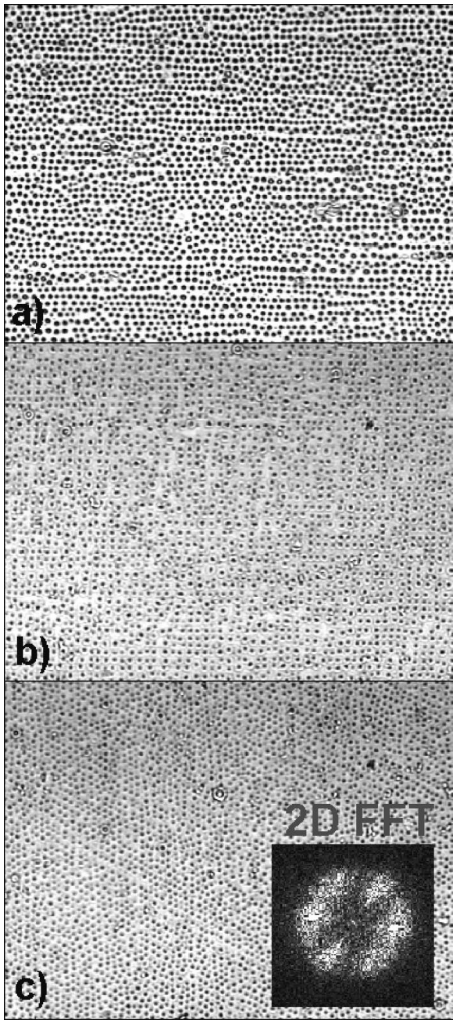

FIG. 10. Orientation of the morphology is possible. This is achieved by rubbing the substrate prior to spin coating the polymer films. Data are shown for (a) lines (b) squares, and (c) hexagonally packed arrays.

the equilibrium volume fraction of water and a corresponding increase in the in-plane swelling strain. This allows the film to buckle with greater amounts of curvature and pushes the blistering length to smaller values.

Depth of craters

As well as measuring the diameter of the craters, an AFM was used to image the topology of the samples. This revealed that the craters were typically 10–100 nm deep and that the depth of the crater could be controlled by changing the film thickness. The crater depth as a function of film thickness for samples immersed in water at 40 °C for 5 min is shown in Fig. 9. The two quantities plotted in this graph represent the distance between the top of the crater and the base, h_{tb}, and the distance between the top surface of the undetached areas of the film and the base of the crater, h_{fb}. This second quantity is nonzero, indicating that the detached parts of the film experience some viscous flow and that thinning of the film occurs. Thus, when the films are removed from the water, the

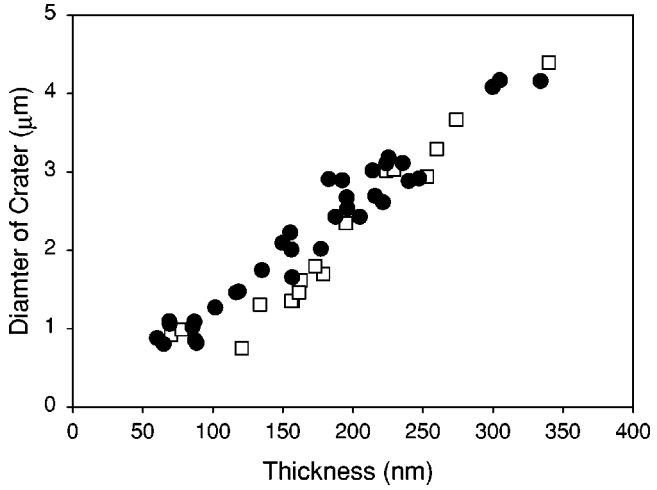

FIG. 11. Orientation of the morphology does not change the blistering length λ. Data are shown for unoriented samples (●) and samples showing the line morphology (□).

blistered part collapses back down to produce a crater that extends below the top surface of the film.

As the temperature of the water is increased, the viscosity of the hydrated film is expected to decrease. This means that the application of a swelling stress will cause more flow in the buckled material and will result in a larger amount of thinning of the buckled part of the film as stress is dissipated. The net result for a given film thickness is a deeper crater [Fig. 8(b)].

Orientation of morphology

It is possible to orient the morphology by rubbing the substrate prior to spin casting of the film. The rubbing described here was performed using a cylindrical velvet coated roller attached to a dc motor.

The orientations achieved are shown in Fig. 10. The line morphology was obtained by simply rubbing the substrate in one direction, the squares by rubbing in two orthogonal directions, and the hexagons by rubbing the substrate twice with a 60° angle between the rubbing directions. Of the three types of morphology, the most technologically interesting are the lines and square arrays. These structures clearly show long range order while the hexagonal ordering decays over much shorter distances.

There is no change in crater size due to the effects of rubbing the substrate (see Fig. 11); instead it is believed that rubbing simply introduces some anisotropy into the adhesive properties of the substrate [23].

CONCLUSIONS

The swelling of a polymer film confined by a substrate can lead to an osmotically driven blistering process. These blisters form with some characteristic blistering length λ, which is controlled by a balance between the membrane stresses in the film, the bending stresses in the blistered film, and the adhesion between the film and the substrate. The membrane stresses in the system are caused by the swelling

of the confined film and the resulting strain can be written in terms of the equilibrium volume fraction of solvent in the polymer. In this study, the swelling strain resulted in blistering on the micrometer length scale. The removal of the blisters from water results in their collapse to produce a monodisperse distribution of craters that are micrometers in diameter and are between 10 and 100 nm deep.

It is possible to align these craters by simply rubbing the substrate before the polymer film is deposited. There is no apparent change in the crater dimensions due to this process and it is believed to occur simply as a result of anisotropic adhesion caused by the modification of the substrate by the rubbing process. The ability to align monodisperse objects that self-assemble with dimensions in the ranges of micrometers and tens of nanometers is potentially very exciting for a number of applications.

The theories used to describe blister formation and growth indicate that this phenomenon should be observable in other systems. This would involve finding the correct polymer/solvent/substrate system. In this study, the equilibrium solvent volume fraction in the polymer was shown to influence the initial swelling strain in the films and the viscosity of the polymer. These are the physical properties that are responsible for controlling the initial blistering length λ and the growth time τ_0 of the blisters, respectively. The solvent volume fraction is clearly an easy parameter to control, because for a given polymer a suitable solvent can usually be found that swells the polymer by the required amount to produce the strain required. However, the parameter that is not easy to control is the energetics of the surface interaction between the swollen polymer and the substrate. This determines if the polymer will detach from the substrate and if the resulting blisters will grow. By choosing a system where the surface interaction can be tuned, it may be possible to produce these structures using more ''processing friendly'' materials.

ACKNOWLEDGMENTS

We would like to thank Professor K. R. Shull for useful discussions during the course of this work and Dr. K. S. Whitehead for the use of the rubbing apparatus. We would also like to thank AstraZeneca (U.K.) Ltd., Avecia Ltd., and Syngenta for supporting this work as part of their strategic research fund and particularly Jonathan Booth for supplying the materials.

[1] M. Srinivasarao, D. Collings, A. Phillips, and S. Patel, Science **292**, 79 (2001).
[2] A. M. Higgins and R. A. L. Jones, Nature (London) **404**, 476 (2000).
[3] K. Dalnoki-Veress, B. G. Nickel, and J. R. Dutcher, Phys. Rev. Lett. **82**, 1486 (1999).
[4] E. Schäffer, T. Thurn-Albrecht, T. P. Russell, and U. Steiner, Nature (London) **403**, 874 (2000).
[5] V. Shenoy and A. Sharma, Phys. Rev. Lett. **86**, 119 (2001).
[6] M. Ibn-Elhaj and M. Schadt, Nature (London) **410**, 796 (2001).
[7] T. J. Chuang, T. Nguyen, and S. Lee, J. Coatings Technol. **71**, 75 (1999).
[8] H. Gleskova, S. Wagner, and Z. Suo, Appl. Phys. Lett. **75**, 3011 (1999).
[9] J. Menčík, *Mechanics of Components with Treated or Coated Surfaces* (Klumer Academic, London, 1967).
[10] G. Gioia and M. Ortiz, Adv. Appl. Mech. **33**, 119 (1997).
[11] M. Ortiz and G. Gioia, J. Mech. Phys. Solids **42**, 531 (1994).
[12] Y. Pomeau, Philos. Mag. B **78**, 235 (1998).
[13] A. L. Ruoff, E. J. Kramer, and C. Li, IBM J. Res. Dev. **32**, 631 (1988).
[14] R. P. Feynman, R. B. Leighton, and M. Sands, *The Feynman Lectures on Physics: Part II* (Addison-Wesley, Reading, MA, 1979).
[15] L. G. Jaeger, *Elementary Theory of Elastic Plates* (Pergamon Press, Oxford, 1964).
[16] S. P. Timoshenko, *Theory of Plates and Shells*, 2nd ed. (McGraw-Hill, New York, 1959).
[17] S. P. Timoshenko and J. Gere, *Theory of Elastic Stability* (McGraw-Hill, New York, 1961).
[18] H. G. Allen, *Analysis and Design of Structural Sandwich Panels* (Pergamon Press, Oxford, 1969).
[19] N. Bowden, S. Brittain, A. G. Evans, J. W. Hutchinson, and G. Whitesides, Nature (London) **393**, 146 (1998).
[20] J. Menčík, Ceram. Silikáty **36**, 93 (1991).
[21] R. A. L. Jones and R. W. Richards, *Polymers at Surfaces and Interfaces* (Cambridge University Press, Cambridge, England, 1999).
[22] K. Q. Xia, C. Franck, and B. Widom, J. Chem. Phys. **97**, 1446 (1992).
[23] J. A. Castellano, *Liquid Crystals and Ordered Fluids* (Plenum, New York, 1984), Vol. 4, pp. 763–780.